Nano World Journal

https://doi.org/10.17756/nwj.2023-s2-079

Research Article

Open Access

Use of Natural Phosphate as Alternative Adsorbent for Water Depollution

Ikrame Es-saidi, Jihane Labrag, Meryem Abbadi, Abdeladim Ouguidoum and Abdelaziz Laghzizil*

Laboratory of Applied Chemistry of Materials, Faculty of Science, Mohammed V University in Rabat, Avenue Ibn Batouta BP.1014, Rabat Morocco

***Correspondence to:**

Abdelaziz Laghzizil
Laboratory of Applied Chemistry of Materials,
Faculty of Science,
Mohammed V University in Rabat,
Avenue Ibn Batouta BP.1014,
Rabat Morocco.
E-mail: laghzizi@fsr.ac.ma

Received: July 25, 2023
Accepted: September 27, 2023
Published: September 29, 2023

Citation: Es-saidi I, Labrag J, Abbadi M, Ouguidoum A, Laghzizil A. 2023. Use of Natural Phosphate as Alternative Adsorbent for Water Depollution. *NanoWorld J* 9(S2): S466-471.

Copyright: © 2023 Es-saidi et al. This is an Open Access article distributed under the terms of the Creative Commons Attribution 4.0 International License (CCBY) (http://creativecommons.org/licenses/by/4.0/) which permits commercial use, including reproduction, adaptation, and distribution of the article provided the original author and source are credited.

Published by United Scientific Group

Abstract

Heavy metals are found in the effluents of many industrial units. The applicability of Moroccan natural phosphate from Benguerir (NPB) and Khouribga (NPK) regions can remove some heavy metals from water. This approach is considered benefic, inexpensive, and very effective for the treatment of contaminated waters. The raw samples of NPB and NPK are mainly composed of carbonated fluorapatite (FAP) associated with some impurities such as SiO_2 and CaF_2. The heat treatment of these materials at 600 °C, 800 °C, and 1000 °C results in a single crystalline phase of phosphosilicate apatite. First, the adsorption efficiency of the dried phosphates depends on their mineralogy on the nature of the metal (Pb^{2+}, Cd^{2+}, Zn^{2+}, and Cr^{3+}) in the order $Pb^{2+} > Cr^{3+} > Cd^{2+} > Zn^{2+}$. After treatment at 600 °C and 800 °C, the adsorption efficiency of the selected NPB sample was tested against Cr^{3+} and Cd^{2+} ions and it was slightly better compared to the raw sample. Therefore, NPB heat-treated at 600 °C can be considered a stable adsorbent and depollution agent for wastewaters.

Keywords

Natural adsorbents, Heavy metals treatment, Removal efficiency, Water depollution

Introduction

The development of low-cost adsorbents has led to a rapid growth of research interests in this area. On an industrial scale, pollutants are removed from water using columns and contractors filled with suitable natural adsorbents [1-3]. This adsorption technology has been widely used for water purification by developing nanoscale adsorbent alternatives to activated carbon based on performance, adsorption efficiency and cost [4]. For this, many reflections have been carried out on the use of geomaterials and natural biomass as well their derived products, which are abundant and more respectful of the environment, such as clays [5, 6], zeolites [7], fly ashes [8], shales [9], biomasses [10]. Phosphate is a natural resource with multiple uses, in particular to produce phosphoric acid and fertilizers [11, 12]. Natural phosphates appear of great interest related to their chemical characteristics with a main crystalline structure isomorphic to FAP $Ca_{10}(PO_4)_6F_2$ [13, 14], but their chemical composition varies from one geological site to another.

Phosphate rock can be a suitable adsorbent for the majority of pollutants, but it is desirable to be treated or activated to release active sites and stabilize associated impurities. Interest in the contamination of environmental media (Water and soil) by metal ions is growing due to their undesirable effect on the health of living beings, and on the imbalance of ecosystems. Several remediation techniques have been discussed to remedy surface waters and soils [15, 16] requiring

a large amount of adsorbent, which is always pushed to use natural phosphate thanks to their abundance in nature at low cost compared to other treatment agents [17]. The presence of P-OH groups in raw or modified natural phosphate has a structuring and inductive function to have very interesting surface properties. Natural and synthetic apatites have attracted the attention of several researchers for their intense applications as heterogeneous catalysts [18, 19], adsorbents and ion exchangers [13, 20, 21]. The most common and widely used type of natural phosphate in Morocco is sedimentary characterized by its reactivity and the easy production of its components as well as the high content of P_2O_5.

Materials and Method

The thermal and chemical treatment of these ores makes it possible to control their chemical composition by mainly degrading the carbonates, which can give these minerals a more adsorbent character. In this work, two Moroccan phosphates from the Benguerir (NPB) and Khouribga (NPK) regions were sampled. Their characterization in raw and modified state is carried out using different techniques capable of identifying their structural and morphological properties. Their surface property was evaluated for the removal of certain metal ions (Pb^{2+}, Cd^{2+}, Zn^{2+}, and Cr^{3+}) from water. Some parameters that affect the metal ion adsorption process have been discussed. All used materials are nanoscale materials.

Results and Discussion

Characterization studies

The XRD (X-ray diffraction) examination of the samples was carried out using a PAnalytical X'Pert Pro powder diffractometer, using copper K_α radiation (λ = 1.5406 Å). The data was collected in the interval 2θ(°), 10 - 80° with a step of 0.02°/s. Figure 1 shows the diffractograms of natural phosphates studied showing fine lines related to the different crystalline phases. First, the analysis of the NPB sample dried at 100 °C shows the presence of the main diffraction lines at diffraction angles (2θ) around 25.84°, 32.13°, 33.34°, and 34.12° attributable to the apatitic phase of space group $P6_3/m$ and correspond respectively to planes (hkl) (002), (211), (300), and (202) (JCPDS 09-0432). In NPK case, these lines are slightly shifted and located around 25.95°, 32.96°, 33.14°, and 34.24°. In addition to the majority apatite phase, the relative quartz-SiO_2 diffraction lines are detected, but more intense in NPB case at 2θ = 26.62°. Other impurities are observed such as calcite ($CaCO_3$) at 2θ = 35.73° and fluorite (CaF_2) around 2θ = 29.35°. Calcite exists in very small quantities while the line of fluorite is overlapped with one of the lines of apatite. Note that the absence of the clay fraction detected in most phosphate deposits, namely palygorskite $(Mg,Al)_5(Si,Al)_8O_{20}(OH)_2(H_2O)_8$ and sanidine ($KAlSi_3O_8$) shows that the treatments carried out beforehand are effective and lead to well-purified and P_2O_5-rich phosphate samples as will be shown later. The presence of these clays strongly affects the quality of the phosphate rock whether in the acid attack to produce H_3PO_4, or generally its surface properties. This mineralogy has also been observed in the Moroccan natural phosphate of Youssoufia (Morocco) as in the majority of foreign phosphate deposits [3, 22]. So, the treatment carried out beforehand can influence the mineralogical characteristics of the final product.

The crystalline parameters a and c of the samples dried at 100 °C and calcined at 1000 °C were compared to those of $Ca_{10}(PO_4)_6F_2$ (FAP) and hydroxyapatite $Ca_{10}(PO_4)_6(OH)_2$ (HAP) indicating that the studied phosphates are mainly composed of a Froncolite, which is a well crystallized carbonated apatite [23]. The difference is due to the presence of certain metals in small quantities incorporated into the apatite matrix (Na^+, K^+, Cd^{2+}, and Mg^{2+}). Similarly, the partial substitution of phosphate groups by carbonates still affects a and c values.

The FTIR (Fourier-transform infrared) spectra were recorded using a Brüker IFS66v FTIR spectrometer in the frequency 400 - 4000 cm^{-1} range with a step of 2 cm^{-1}. They show two regions of intense reflection characteristic of the symmetrical and antisymmetrical vibrations of PO_4 located between 950 - 1100 cm^{-1} and those of deformation between 571 - 601 cm^{-1} (Figure 2). A slight displacement of these bands was observed towards the low frequencies for the NPK compared to the NPB sample related to the nature of elements in the NPK structure. Other bands relating to carbonates at 1458 cm^{-1}, 1430 cm^{-1}, and 871 cm^{-1} were detected. It should be noted that the FTIR spectra of the two phosphate NPB and NPK samples do not show any characteristic absorption band at OH-hydroxyls around 3560 cm^{-1} and 630 cm^{-1}. This confirms that these raw natural phosphates are isomorphic to a carbonated FAP proven by the analysis of fluorine. Bands

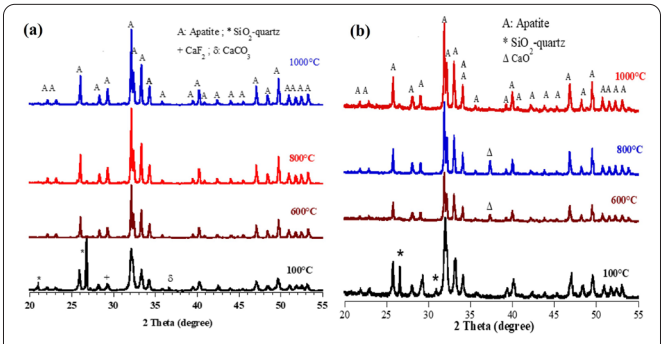

Figure 1: XRD diagrams of natural phosphates **(a)** NPB and **(b)** NPK thermally treated at various temperatures.

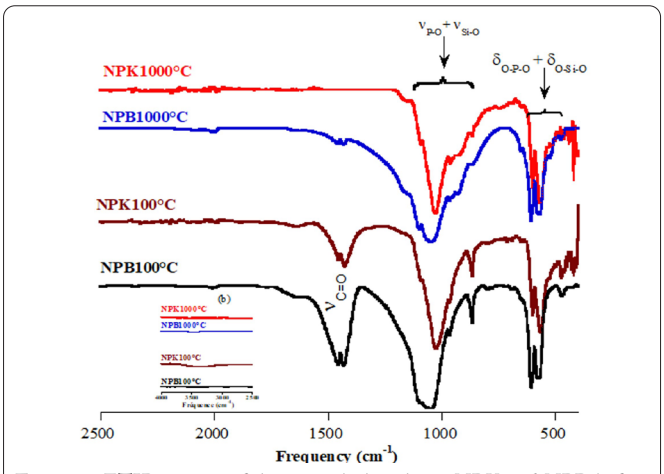

Figure 2: FTIR spectra of the natural phosphates NPK and NPB before and after thermal activation testifying to the absence of the OH bands.

around 2000 - 2500 cm^{-1} of very low intensity are attributed to residual traces of carbonyl compounds. Likewise, the Si-O bands are not well readable because they overlapped with the P-O bands in the same absorption ranges. So, this shows that the two phosphate rocks have the same functional groups.

Since natural phosphate is considered to be a very complex matrix combining several mineral and organic chemical constituents, thermal analysis involves numerous reactions of desorption of volatile compounds and combustion of resistant entities with specific mechanisms for each step. The TG (Thermogravimetric) analysis shows the presence of three main thermal events and each thermal phenomenon is therefore the site of different chemical reactions (Figure 3). From ambient temperature to 200 °C, there is water desorption. Compared to NPB powder, the water retained by the surface of NPK is greater, indicating that the latter is more hydrophilic. From 200 °C to 600 °C, there is a decomposition of certain organic and carbonated materials which are not directly linked to the apatitic network whose mass losses obtained in this temperature range are comparable in the two phosphates. Beyond 600 °C, carbonates linked to the structure of the apatite are degraded and the mass losses are clearly different, indicating that the NPK phosphate contains more carbonates than the NPB.

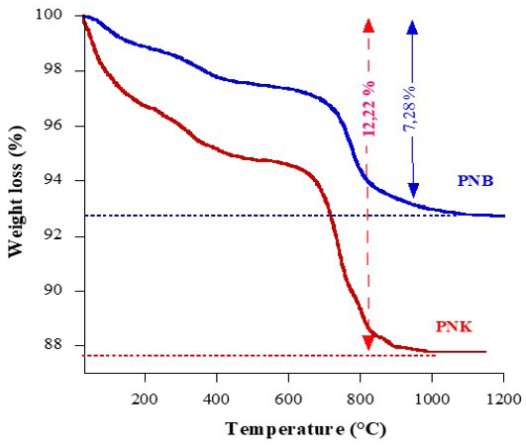

Figure 3: TG analysis of dried NPB and NPK rock phosphates.

The main chemical elements present in the prepared materials were analyzed by X-ray fluorescence (Table 1). The Ca/P molar ratio of NPB dried at 100 °C is about 1.97, which is slightly higher than that of NPK (1.84) and of pure FAP $Ca_{10}(PO_4)F_2$ (Ca/P=1.667). This difference is due to carbonates and other impurities present in the ore, as shown by XRD and FTIR data. It can be seen that the Ca/P molar ratios of the two NPB and NPK phosphates dried at 100 °C are different, whereas those calcined are almost the same, but slightly higher than that of a stoichiometric FAP (Ca/P = 1.667).

The difference obtained is due to the existence of some elements inserted into the FAP matrix such as silicates. As shown in Table 2, the fluorine and silicon contents depend on the source of the phosphate. The heat treatment at 1000 °C reduced the fluorine amount in the calcined materials as reported elsewhere [24].

The N_2-sorption isotherms of at 77 K on the NPB and

Table 1: Crystalline parameters a and c of dried and calcined NPB and NPK matrices compared to the pure FAP and HAP demonstrating crystal volume distortion of apatite structure.

	NPB		NPK		FAP	HAP
	100 °C	1000 °C	100 °C	1000 °C		
(a ±0,004) (Å)	9.360	9.393	9.363	9.387	9.372	9.421
(c ±0,002) (Å)	6.889	6.882	6.882	6.883	6.888	6.882

Table 2: Chemical analyses of the main chemical elements of fire and calcined NPK and NPB materials.

		Ca (%)	P (%)	Si (%)	F (%)	Ca/P
NPB	100 °C	37.84	15.03	1.78	3.07	1.945
	600 °C	35.55	15.82	1.84	2.92	1.736
	1000 °C	35.40	15.81	1.85	2.80	1.730
NPK	100 °C	36.87	15.51	1.85	2.81	1.836
	600 °C	35.82	15.78	1.92	2.72	1.747
	1000 °C	35.75	15.80	1.94	2.41	1.740

NPK powders at 100 °C show type IV hysteresis loops according to the IUPAC classification, which indicates that the powders are mesoporous (Figure 4). The calculated specific surfaces areas of NPB and NPK powders dried at 100 °C are 20 m^2g^{-1} and 25 m^2g^{-1}, respectively while those of the products calcined at 800 °C are dramatically reduced to 5 m^2g^{-1} and 8 m^2g^{-1} suggesting that after full degradation of the organic matter, mineral grain coarsening has occurred.

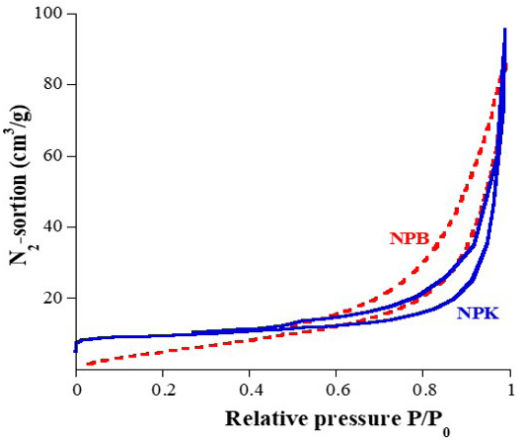

Figure 4: N_2-adsorption/desorption isotherms on NPB and NPK powders dried at 100 °C.

Surface charge powders

The control of the acid-base behavior of NPB and NPK surfaces makes it possible to characterize the charges involved and consequently their reactivity versus the adjacent species. The evolution of the equilibrium pH as a function of time of aqueous solutions containing in suspensions of NPB and NPK steamed at 100 °C and calcined at 600 °C are plotted in Figure 5a. A gradual increase in the pH of the solutions monitored is observed, followed by a plateau where the equilibrium pH value depends on the phosphate mineralogy and the heat treatment carried out. This pH increase is due to the release of

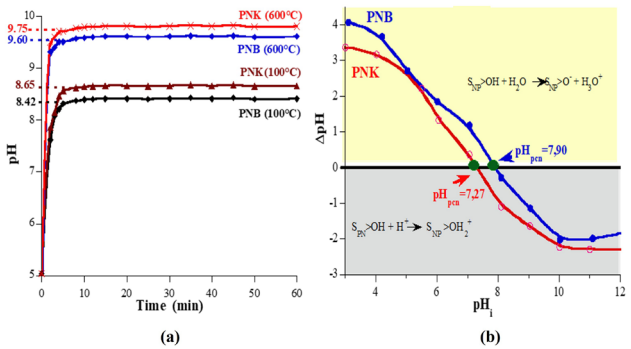

Figure 5: Kinetics of the pH evolution of the dried and calcined NPB and NPK suspensions in water and isoelectric points of their dried surfaces.

some basic species into the solution or to a protonation of the solid surface. It is also noted that the equilibrium pH of the NPK suspensions is higher than that of NPB and also increases with heat treatment. This may possibly be linked to the phenomenon of wetting of the phosphate surface, which becomes capable of fixing protons via a proton exchange mechanism. The heat treatment of powder at 600 °C or 800 °C promotes this exchange via the decomposition of carbonates and organic molecules and can subsequently activate the process of retention of antagonistic species.

The acid-base behavior of a mineral surface is further characterized by its point of zero charge, which is an essential parameter for predicting its interactions with neighboring charged entities. In aqueous solutions, the NPB and NPK particles develop antagonistic surface charges which can be hydrated according to the surface species, which affects the pH of the medium. The point of zero charge of the solid surface "S_{NP}>" is tested experimentally by potentiometric titration according to acid/base reactions [25] The pH_{pzc} value is the pH of the solution for which the net global charge vanishes, i.e., the quantities $S_{NP} > OH_2^+$ and $S_{NP} > O^-$ are equal according to the following reactions:

$$S_{NP} > -OH + H^+ \rightarrow SNP > OH_2^+ ; S_{NP} > -OH + H_2O \rightarrow S_{NP} > -O^- + H_3O^+$$

The pH_{pzc} values of the NPB and NPK samples are 7.90 and 7.27, respectively (Figure 5b), which are close to those of pure fluorapatite (pH_{pzc} = 7.00) and hydroxyapatite (pH_{pzc} = 7.50) reported in the literature [26] where the difference observed is related to the carbonate content containing in each natural phosphate. According to these values and the mineralogy of each natural phosphate studied, the sorption of metal ions must take place at acidic pH according to the mineralogy of each natural phosphate studied.

Surface properties

The main purpose of this part is to understand the effect of rock phosphate mineralogy on its metal adsorption properties. Aqueous solutions of Pb^{2+}, Cd^{2+}, Zn^{2+}, and Cr^{2+} ions at different concentrations were prepared respectively from the salts ($Pb(NO_3)_2.xH_2O$), ($Cd(NO_3)_2.xH_2O$), ($Pb(NO_3)_2$), and $Cr(NO_3)_3.6H_2O$. The adsorption kinetics were checked by adding 200 mg of powder to 100 ml of the metal solution at 100 mg/L at 22 °C under magnetic stirring. The pH was adjusted to 5 by adding aqueous solutions of 1 M NaOH or 1 N HCl. For each instantaneous sample, the suspension is filtered and the residual metal in the filtrate is analyzed by atomic absorption spectroscopy. The instantaneous quantity of adsorbed metal q_t (mg/g) is determined according to the following equation: $q_t = \frac{C_0 - C_t}{m}.V$, where C_0 and C_t are the initial concentrations and at time "t" in metal ions (mg/L) in the solution, respectively. m (g) is the mass of the adsorbent in the solution and V(L) is the volume of the contaminated solution. All tests were done in triplicate and the experimental error is less than 5%.

Figure 6 shows the adsorption kinetics of Pb^{2+}, Cd^{2+}, Zn^{2+}, and Cr^{2+} on NPB and NPK dried at 100 °C under specific conditions. The equilibrium times of the adsorption process differ according to the nature of the metal and the adsorbent (Table 3). This difference is linked to the nature of the active sites and to electrostatic metal-phosphate interactions. Due to the similar retention of Cd^{2+} and Cr^{3+} ions, Pb^{2+} ions are almost completely adsorbed on NPB and NPK while Zn^{2+} ions are less adsorbed than other metals.

In order to study the effect of carbonates and organic matter in natural phosphate, we tested the adsorption efficiency of NPB calcined at 600 °C and 800 °C against Cd^{2+} and Cr^{3+} ions (Figure 7).

Adsorption curves show the same pattern and are characterized by a high rate of elimination of Cr^{3+} by NPB600 (92.4%) slightly higher than that of Cd^{2+} ions with 100 ppm as initial concentration (Table 4). The removal of Cr^{3+} and Cd^{2+} ions by NPB is related to their charge and the nature of the interactions of each ion with the NPB surface depending on its heat treatment state. The best adsorption efficiency was obtained at 600 °C for both metals. This is due to a synergy

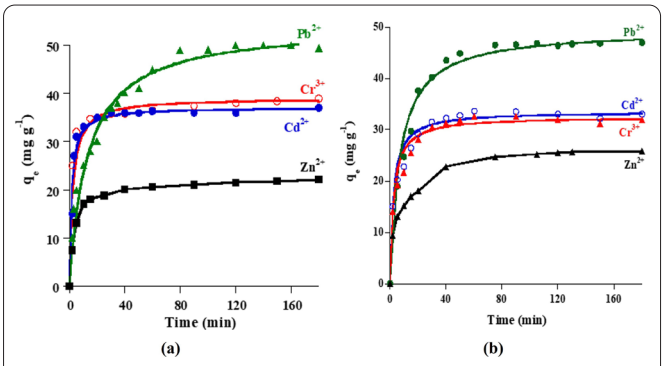

Figure 6: Effect of incubation time on metal adsorption on **(a)** NPB and **(b)** NPK. (C_0 = 100 ppm, pH = 5, dose = 2 g/L, and T = 22 °C).

Table 3: Adsorption capacities and equilibrium times for the retention of different metals by dried NPB and NPB adsorbents.

		Pb^{2+}	Cd^{2+}	Zn^{2+}	Cr^{3+}
NPB	$q_{e,max}$ (mg/g)	49.95	36.06	22.20	38.10
	Removal (%)	99.00	72.1	44.00	76.20
	Equilibrium time (min)	60.00	25.0	50.00	90.00
NPK	$q_{e,max}$ (mg/g)	46.65	33.46	25.70	32.21
	Removal (%)	93.30	66.92	26.40	64.42
	Equilibrium time (min)	45.00	60.0	75.00	60.00

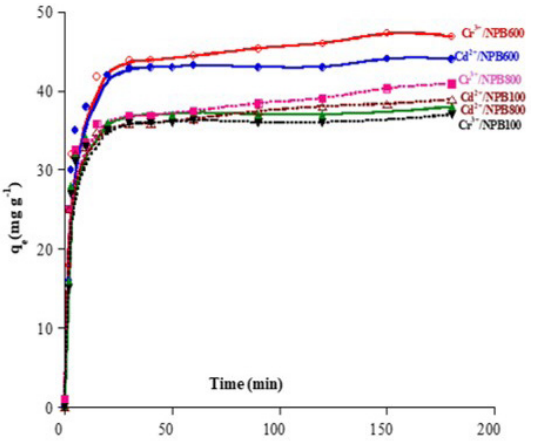

Figure 7: Effect of heat treatment of NPB powder at 600 °C and 800 °C on its ability to retain Cr^{3+} and Cd^{2+} ions showing the effect of decomposed species after thermal treatment (C_0 = 100 mg/L, pH = 5, dose = 2 g/L, and T = 24 °C).

between the decomposition of carbonates and/or organic matter thus blocking the apatite network and the release of the dominant active sites P-OH in addition to the crystal growth of the grains. Unlike ionic carbonates in solution which can precipitate metals, carbonates bound to the structure of apatite weaken phosphate-metal interactions. Consequently, their decomposition improves the adsorption efficiency of the phosphate matrix versus the Cr^{3+} and Cd^{2+} ions.

During the sorption reactions, the exchange of protons decreases, and the P-OH or Si-OH groups present on the surface of the NPB become negatively charged (pH > pKa) [27]. All metal ions can be adsorbed on the deprotonated active sites. In fact, Cr^{3+} exists mainly in aqueous medium in the form of Cr^{3+}, $Cr(OH)_2^+$, and $Cr(OH)^{2+}$, which can be easily fixed on the electronegative surface of apatite particles [28]. Based on the results of mineralogy and surface functional groups, calcined NPB at 600 °C contains more P-OH groups which react with Cr^{3+} and Cd^{2+} ions in aqueous solutions. It is therefore advantageous for the heat-treated natural phosphate to have a good affinity for the Cr^{3+} and Cd^{2+} ions.

Table 4: Adsorption characteristics of treated NPB powder.

	Cd^{2+}			Cr^{3+}		
	NPB 100	NPB 600	NPB 800	NPB 100	NPB 600	NPB 800
$q_{e,max}$ (mg/g)	36.06	43.67	36.7	38.10	46.2	40.18
Removal (%)	72.10	87.34	73.40	76.20	92.40	80.36
Equilibrium time (min)	25.0	29.6	30.5	90.0	90.0	88.0

Conclusion

Mineralogical and structural studies of two natural phosphates from Benguerir (NPB) and Khouribga (NPK) regions were carried out in order to define the characteristics of these ores. The combination of all these analytical techniques allows us to interpret the main dissolution and adsorption results. Heat treatment of these phosphates at 600 °C, 800 °C, and 1000 °C affected the mineralogy and associated impurities. The use of these raw and used materials is very effective in the removal of heavy metals (Pb^{2+}, Cd^{2+}, Zn^{2+}, and Cr^{3+}) in water. The degradation mainly of the carbonates contained in the natural phosphates studied slightly improves this metal removal from water.

Acknowledgements

None.

Conflict of Interest

None.

References

1. Abdel-Halim SH, Shehata AMA, El-Shahat MF. 2003. Removal of lead ions from industrial waste water by different types of natural materials. *Water Res* 37(7): 1678-1683. https://doi.org/10.1016/S0043-1354(02)00554-7
2. Hanzlik P, Jehlicka J, Weishauptova Z, Sebek O. 2004. Adsorption of copper, cadmium and silver from aqueous solutions onto natural carbonaceous materials. *Plant Soil Environ* 50(6): 257-264.
3. Mouflih M, Aklil A, Sebti S. 2005. Removal of lead from aqueous solutions by activated phosphate. *J Hazard Mater* 119(1-3): 183-188. https://doi.org/10.1016/j.jhazmat.2004.12.005
4. Miranda LS, Ayoko GA, Egodawatta P, Goonetilleke A. 2022. Adsorption-desorption behavior of heavy metals in aquatic environments: influence of sediment, water and metal ionic properties. *J Hazard Mater* 421: 126743. https://doi.org/10.1016/j.jhazmat.2021.126743
5. Sari A, Tuzen M, Citak D, Soylak M. 2007. Equilibrium, kinetic and thermodynamic studies of adsorption of Pb(II) from aqueous solution onto Turkish kaolinite clay. *J Hazard Mater* 149(2): 283-291. https://doi.org/10.1016/j.jhazmat.2007.03.078
6. Wu Y, Zhang S, Guo X, Huang H. 2008. Adsorption of chromium (III) on lignin. *Bioresour Technol* 99(16): 7709-7715. https://doi.org/10.1016/j.biortech.2008.01.069
7. Andrejkovičová S, Sudagar A, Rocha J, Patinha C, Hajjaji W, et al. 2016. The effect of natural zeolite on microstructure, mechanical and heavy metals adsorption properties of metakaolin based geopolymers. *Appl Clay Sci* 126: 141-152. https://doi.org/10.1016/j.clay.2016.03.009
8. Duan P, Yan C, Zhou W, Ren D. 2016. Development of fly ash and iron ore tailing based porous geopolymer for removal of Cu(II) from wastewater. *Ceram Int* 42(12): 13507-13518. https://doi.org/10.1016/j.ceramint.2016.05.143
9. Gouza A, Saoiabi S, El Karbane M, Masse S, Laurent G, et al. 2017. Oil shale powders and their interactions with ciprofloxacin, ofloxacin, and oxytetracycline antibiotics. *Environ Sci Pollut Res* 24: 25977-25985. https://doi.org/10.1007/s11356-017-0100-5
10. Saralegui AB, Willson V, Caracciolo N, Piol MN, Boeykens SP. 2021. Macrophyte biomass productivity for heavy metal adsorption. *J Environ Manag* 289: 112398. https://doi.org/10.1016/j.jenvman.2021.112398
11. Dybowska A, Manning DA., Collins MJ, Wess T, Woodgate S, et al. 2009. An evaluation of the reactivity of synthetic and natural apatites in the presence of aqueous metals. *Sci Total Environ* 407(8): 2953-2965. https://doi.org/10.1016/j.scitotenv.2008.12.053
12. Bouyarmane H, El Hanbali I, El Karbane M, Rami A, Saoiabi A, et al. 2015. Parameters influencing ciprofloxacin, ofloxacin, amoxicillin and sulfamethoxazole retention by natural and converted calcium phosphates. *J Hazard Mater* 291: 38-44. https://doi.org/10.1016/j.jhazmat.2015.02.049
13. Bahdod A, El Asri S, Saoiabi A, Coradin T, Laghzizil A. 2009. Adsorption of phenol from an aqueous solution by selected apatite adsorbents: kinetic process and impact of the surface properties. *Water Res* 43(2): 313-318. https://doi.org/10.1016/j.watres.2008.10.023

14. Ettoumi M, Jouini M, Neculita CM, Bouhlel S, Coudert L, et al. 2020. Characterization of Kef Shfeir phosphate sludge (Gafsa, Tunisia) and optimization of its dewatering. *J Environ Manag* 254: 109801. https://doi.org/10.1016/j.jenvman.2019.109801

15. Chen SB, Zhu YG, Ma YB. 2006. The effect of grain size of rock phosphate amendment on metal immobilization in contaminated soils. *J Hazard Mater* 134(1-3): 74-79. https://doi.org/10.1016/j.jhazmat.2005.10.027

16. Cao X, Wahbi A, Ma L, Li B, Yang Y. 2009. Immobilization of Zn, Cu, and Pb in contaminated soils using phosphate rock and phosphoric acid. *J Hazard Mater* 164(2-3): 555-564. https://doi.org/10.1016/j.jhazmat.2008.08.034

17. El Asri S, Laghzizil A, Coradin T, Saoiabi A, Alaoui A, et al. 2010. Conversion of natural phosphate rock into mesoporous hydroxyapatite for heavy metals removal from aqueous solution. *Colloids Surf A Physicochem Eng Asp* 362(1-3): 33-38. https://doi.org/10.1016/j.colsurfa.2010.03.036

18. Gruselle M. 2015. Apatites: a new family of catalysts in organic synthesis. *J Organomet Chem* 793: 93-101. https://doi.org/10.1016/j.jorganchem.2015.01.018

19. Gruselle M, Tonsuaadu K, Gredin P, Len C. 2022. Apatites based catalysts: a tentative classification. *Mol Catal* 519: 112146. https://doi.org/10.1016/j.mcat.2022.112146

20. Thomann JM, Gasser P, Bres EF, Voegel JC, Gramain P. 1990. Development of an automated experimental setup for the study of ionic-exchange kinetics. Application to the ionic adsorption, equilibrium attainment and dissolution of apatite compounds. *Comput Methods Programs Biomed* 31(2): 89-95. https://doi.org/10.1016/0169-2607(90)90055-E

21. El Bekkali C, Bouyarmane H, Saoiabi S, El Karbane M, Rami A, et al. 2016. Low-cost composites based on porous titania–apatite surfaces for the removal of patent blue V from water: effect of chemical structure of dye. *J Adv Res* 7(6): 1009-1017. https://doi.org/10.1016/j.jare.2016.05.001

22. Aouad A, Benchanâa M, Mokhlisse A, Arafan A. 2002. Study of thermal behaviour of organic matter from natural phosphates (Youssoufia-Morocco). *J Therm Anal Calorim* 70(2): 593-603. https://doi.org/10.1023/a:1021601329760

23. Vignoles-Montrejaud M, Bonel G, Bacquet G. 1982. Étude physico-chimique des apatites carbonatées phospho-calciques semblables à la francolite. *Bull Miner* 105(3): 307-311.

24. Laghzizil A, Elhrech N, Britel O, Bouhaouss A, Ferhat M. 2000. Removal of fluoride from Moroccan phosphate and synthetic fluoroapatites. *J Fluorine Chem* 101(1): 69-73. https://doi.org/10.1016/S0022-1139(99)00184-0

25. Ahmad R, Kumar R, Haseeb S. 2012. Adsorption of Cu^{2+} from aqueous solution onto iron oxide coated eggshell powder: evaluation of equilibrium, isotherms, kinetics, and regeneration capacity. *Arab J Chem* 5(3): 353-359. https://doi.org/10.1016/j.arabjc.2010.09.003

26. Harding IS, Rashid N, Hing KA. 2005. Surface charge and the effect of excess calcium ions on the hydroxyapatite surface. *Biomaterials* 26(34): 6818-6826. https://doi.org/10.1016/j.biomaterials.2005.04.060

27. Elouear Z, Bouzid J, Boujelben N, Feki M, Jamoussi F, et al. 2008. Heavy metal removal from aqueous solutions by activated phosphate rock. *J Hazard Mater* 156(1-3): 412-420. https://doi.org/10.1016/j.jhazmat.2007.12.036

28. Achelhi K, Masse S, Laurent G, Roux C, Laghzizil A, et al. 2011. Ultrasound-assisted synthesis of mesoporous zirconia-hydroxyapatite nanocomposites and their dual surface affinity for Cr^{3+}/$Cr_2O_7^{2-}$ions. *Langmuir* 27(24): 15176-15184. https://doi.org/10.1021/la2029643